# STITCHED COMPOSITES WITH THREE-DIMENSIONAL STITCH PATHS

Andrew E. Lovejoy, Dawn C. Jegley
NASA Langley Research Center
Hampton, VA/USA

## ABSTRACT

Stitched composites have been shown to exhibit damage tolerance and to reduce weight compared to traditional layered composites through unitization of the structure by elimination of fasteners. Stitching capabilities have been incorporated into the Integrated Structural Assembly of Advanced Composites (ISAAC) system at NASA Langley Research Center with the introduction of two stitching heads. Stitching path control was initially implemented as straight lines in space, as was done for previous stitching development. However, more complex stitched structures such as a wind tunnel blade or around cutouts within a fuselage or wing skin, require that the stitching paths be implemented as three-dimensional (3D) stitching paths in space. Unfortunately, control programming output by an existing preprocessor program cannot stitch these curved paths due to problems that arise in stitch formation and the introduction of side forces on the needles using the conventional programming approach whereby the head is simultaneously controlled through translations and rotations. This lack of capability is most significant for the single-sided stitching head, where two needles are in the preform at the same time for the majority of the stitching process. A means to program 3D stitching paths in space was developed whereby the translation and rotation of each stitch were decoupled, thereby eliminating the problems associated with current control programming approach. Using this newly developed stitching path definition and control programming, complex stitching paths have successfully been stitched at the ISAAC facility. The ability to stitch general 3D stitching paths in space enables the use of stitching on more complex parts.

Keywords: Stitched, Composite, Preform
Corresponding author: Andrew E. Lovejoy (Andrew.E.Lovejoy@nasa.gov)

## 1. INTRODUCTION

Composite materials are now commonly used in high-performance, light-weight aerospace structures. Typical composite laminates exhibit very good in-plane properties, but their performance can be limited by their low through-the-thickness properties, such as interlaminar shear and interlaminar tensile strengths. These reduced through-the-thickness properties make such laminates susceptible to the formation of delaminations, which are often caused by impacts

that occur during part assembly or service operations. As a result, laminated composite parts typically undergo costly nondestructive inspections and evaluations prior to insertion into service and during service. These inspections are necessary to evaluate the delamination sizes and locations to determine if a part needs to be repaired, scrapped, or replaced. Therefore, the need to improve the through-the-thickness properties of composite laminates has led to the development of various methodologies to increase these properties.

Through-the-thickness reinforcement methods have been developed in order to increase the resistance of laminated composites to delamination and other forms of impact damage. These methods are grouped into two main categories, namely matrix augmentation or architecture augmentation [Ref. 1]. Matrix augmentation, or toughening, includes rubber toughening, nanoparticle toughening, and carbon nanotube treatments. Architectural augmentation includes stitching, tufting, z-pinning, three-dimensional (3D) weaving/braiding, and needling. Stitching typically consists of one or two threads or yarns that penetrate through the thickness and connect the through-the-thickness reinforcement across the surfaces of the laminate. Stitches are usually through the entire thickness of the laminate, but blind stitching that penetrates through most of the laminate thickness and only connects the through-the-thickness reinforcement across a single surface is possible. Tufting is similar to stitching except that it uses a single thread or yarn that may or may not connect the through-the-thickness reinforcement across one of the laminate surfaces. Z-pinning consists of inserting precured pins through the thickness of the laminate prior to curing. 3D architecture such as 3D weaving and braiding provide through-the-thickness reinforcement incorporated into the composite architecture, and, depending on the architecture can remove some or most of the unidirectionality associated with typical composite constructions. Lastly, needling is a process whereby barbed needles are pressed through a preform, thereby pushing fibers from one layer down through the layer below, and in the process can cause significant damage to the preform fibers. Stitching was chosen by NASA Langley Research Center (LaRC) as a means to address through-the-thickness strength limitations and was extensively studied.

To achieve the goal of reducing the cost of air travel, NASA has pursued the development of technologies needed for future low-cost, light-weight composite structures for commercial transport aircraft. Through-the-thickness reinforcement was selected for study because the use of traditional layered composite material systems requires fasteners to suppress delaminations and to join structural elements, ultimately leading to fastener pull-through problems or heavy pad-ups in the fastener regions. In contrast, through-the-thickness reinforcement can replace these fasteners throughout each integral panel. This unitization eliminates fasteners and their associated holes, which significantly simplifies the assembly process, reduces part-count, and reduces crack initiation and curtails crack growth throughout the life of the aircraft. The through-the-thickness method chosen was to combine stitching with toughened epoxy in a stitched/resin-infused approach. Stitched/resin-infusion has been extensively researched at LaRC since the 1990s, especially through the Advanced Composite Technology (ACT) [Refs. 2-5] and Environmentally Responsible Aviation (ERA) [Refs. 6-16] projects, as a means to improve the performance, reduce the weight, and reduce the fabrication cost of aircraft structures. Placing stitches at discontinuities, such as along flange edges, has been shown to suppress delamination and turn cracks, which increases the design space and leads to lighter designs [Ref. 16]. Additionally, the most recent infusion and cure processes for stitched panels require high temperatures, but only vacuum pressure, which eliminates the need for an autoclave. The use of stitched dry fabric with resin

infusion and oven cure leads to substantial cost savings and eliminates the out-time concerns associated with traditional prepreg. Through these studies, stitched composite structures have been shown to exhibit damage tolerance and to reduce weight through unitization of the structure by elimination of fasteners.

As a consequence of this effort, a stitched graphite-epoxy material system was identified with the potential for reducing the weight and cost of commercial transport aircraft wing structure. By stitching through the thickness of dry carbon fabric and then infusing with epoxy resin, the labor associated with wing cover panel fabrication and assembly can be significantly reduced. By stitching through the thickness of pre-stacked skin and then stitching together stringers, intercostals and spar caps with the skin, the need for mechanical fasteners is almost eliminated. This manufacturing approach reduces part count, and therefore, cost of the structure. At the same time, newer and more novel aircraft configurations have been proposed that can lead to more complex, 3D stitching paths.

Due to efficiencies and benefits of stitched composites, other composite structure applications could also benefit from stitching, such as launch vehicle dry structure, stiffened conformal pressure vessels and wind tunnel blades. Wind tunnel blades for the National Transonic Facility (NTF) [Ref. 17] are of particular interest at LaRC. A wind tunnel blade from the NTF that was part of a study to use automated fiber placement (AFP) to replace the hand-laid NTF blades [Refs. 18-20] is shown in Figure 1. Stitched wind tunnel blades offer a manufacturing option, however, their highly curved surfaces necessitate the ability to stitch curves in three dimensions over continuous paths. The use of 3D stitching paths could facilitate the fabrication of the interior blade spar (Figure 1a) or the complete blade assembly (Figure 1b) as a single unitized structure with improved performance (blade profile to improve aerodynamics and improved damage tolerance, for example). The need for 3D stitching path capability for wind tunnel blades, aircraft structures, spacecraft structures, and other composite structures with highly curved surfaces was the motivation for formal development of the process to define and program these nonlinear stitching paths at LaRC. The remainder of this paper presents an overview of the stitching capabilities at LaRC, the development of the 3D stitching path definitions required to stitch the complex paths, and conclusions related to the stitching path development and definitions.

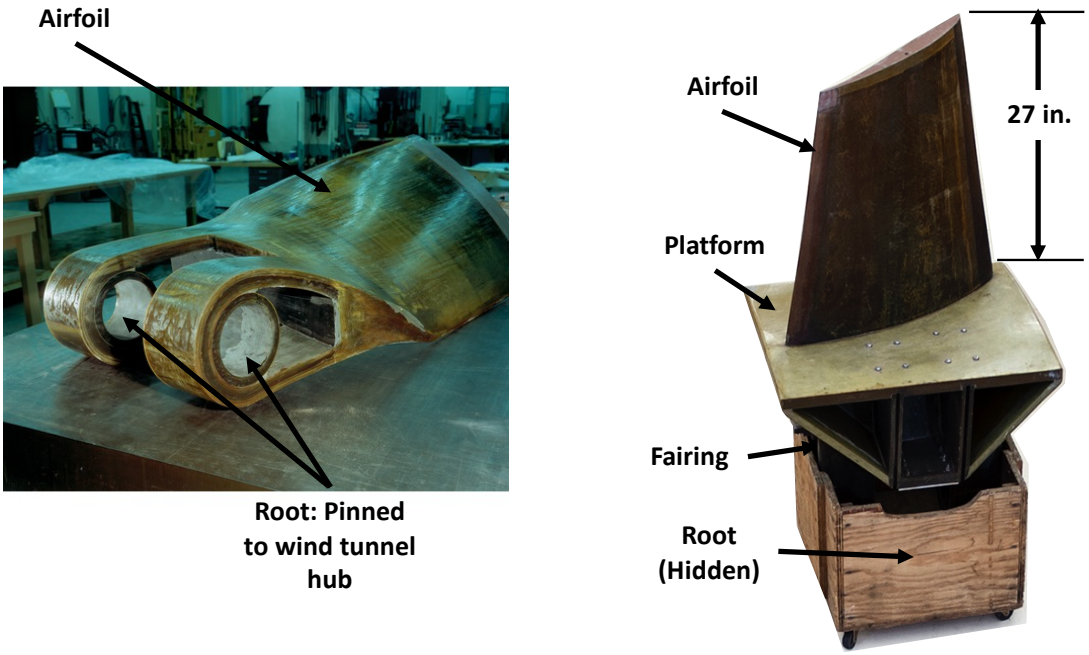


a) Interior blade and spar b) Blade assembly

Figure 1: NTF wind tunnel blade.

## 2. ISAAC FACILITY

Stitching of composite material structures at LaRC is performed at the Integrated Structural Assembly of Advanced Composites (ISAAC) facility. The ISAAC facility houses a robotic system designed to facilitate the development of new technologies related to aerospace composites manufacturing [21]. The robotic system is a six-axis industrial robot capable of accommodating a variety of end effectors. A 41-ft-long linear rail and a vertical rotator provide two additional degrees of freedom. The workcell and operator station are enclosed within an International Organization for Standardization (ISO) Level 7 clean room that provides positive control over airborne particulates and enables consistent temperature and humidity to be maintained. a photograph of the ISAAC robotic system is shown in Figure 2 with the original head capable of performing AFP using up to 16 spools of one quarter-inch wide tows of material. Since the initial installation of the ISAAC facility, several additional heads have been incorporated onto the system to increase functionality.

Because of the success of previous work conducted on stitched composites under LaRC programs, two stitching heads were added to the capabilities of the ISAAC facility to continue development of stitching technology and application to composite structures. Incorporating the stitching heads required coordination between multiple vendors. The stitching end effectors, the machines that perform the stitching process, were manufactured by PFAFF Industriesysteme und Maschinen GmbH Branch Office KSL (KSL)[ϕ] (Lorsch, Germany) through DAP America[ϕ] (Norcross, GA).

[ϕ] The mentioning of a company is not an endorsement by the National Aeronautics and Space Administration (NASA).

The two end effectors comprise a double-sided end effector and a single-sided end effector. The double sided end effector uses one needle and one thread to create a chain stitch to join layers of fabric. The double-sided end effector, termed the RS566 (Figure 3), was primarily an off-the-shell design and requires access to both sides of the preform by the end effector. The single sided end effector uses two needles and one thread to create a modified chain stitch to join layers of fabric that can include more complicated structural arrangements. This single-sided end effector, termed the RS535 (Figure 4), was modified based on past experience with its use during the ERA project and only requires access to one side of the preform by the end effector. Development of the RS535 modifications was facilitated by input from the stitching expert at Boeing that provided stitching development and support throughout the ERA project. LaRC engineers worked with KSL, the needle manufacturer and the Boeing stitching expert, who provided information based upon the experience developed during the ERA project, to develop improvements to the stitching end effector and the catcher needle. The different chain stitch patterns produced by the two stitching heads is shown Figure 5.

The stitching end effectors were incorporated into the ISAAC facility by Electroimpact[ϕ] (EI) (Mukilteo, WA) by joining the stitching end effectors with head plates to create the two stitching heads. In addition, EI provided robot control programming for the ISAAC system. To support that programming, CGTech[ϕ] (Irvine, CA) provided preprocessor capability for the stitching heads in their VERICUT software [22] to enable engineers and technicians to input stitching path geometry to create the G-code, the numerical control code used in computer-controlled manufacturing, for the control system required to perform the stitching operations using the ISAAC robot. Initial implementation of stitching paths in VERICUT was generally limited to straight-line paths, as were used throughout recent stitching development in the ERA project. While VERICUT has the capability to define paths in space, the ability to operate the stitching heads along such paths was not present, and necessitated the development for the logic needed to stitch general paths in three dimensions. Development of these three-dimensional (3D) paths and the associated G-code programming requirements is the focus of this paper, and is presented in the next section.

[ϕ] The mentioning of a company is not an endorsement by the National Aeronautics and Space Administration (NASA).

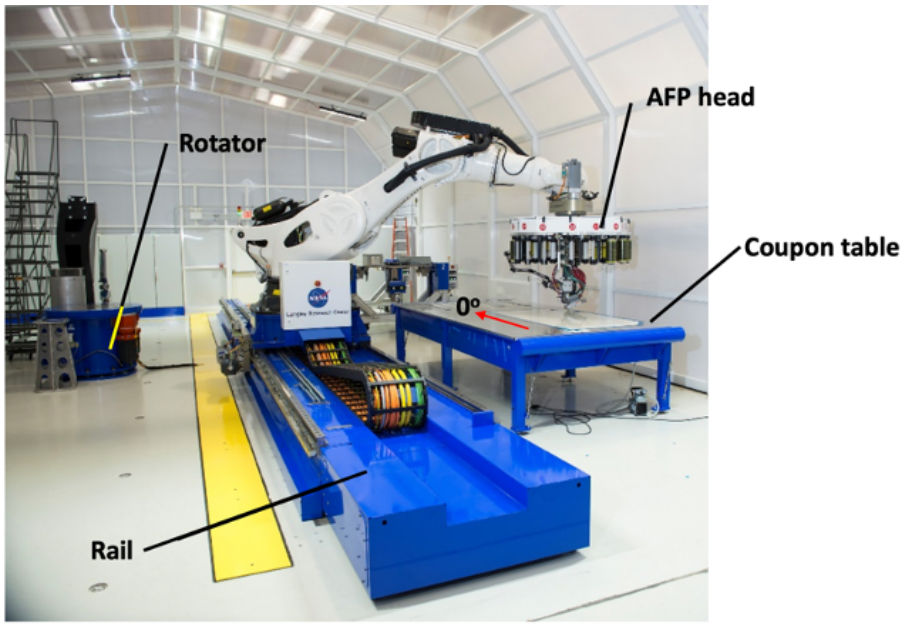


Figure 2: ISAAC robotic system and ISO 7 clean room.

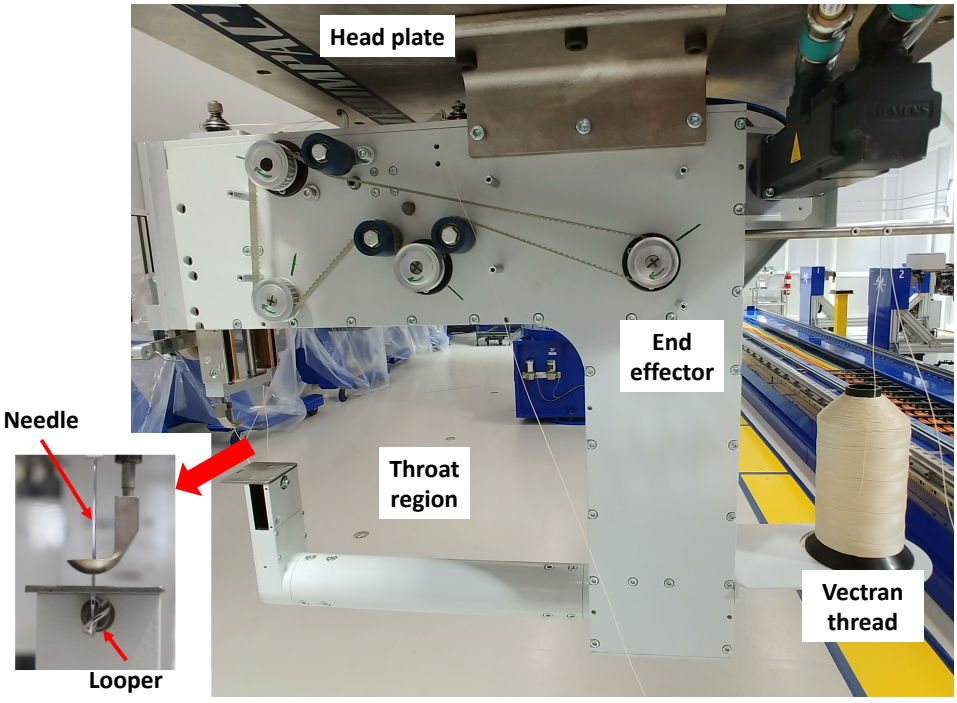


Figure 3. RS566 (double-sided) stitching head.

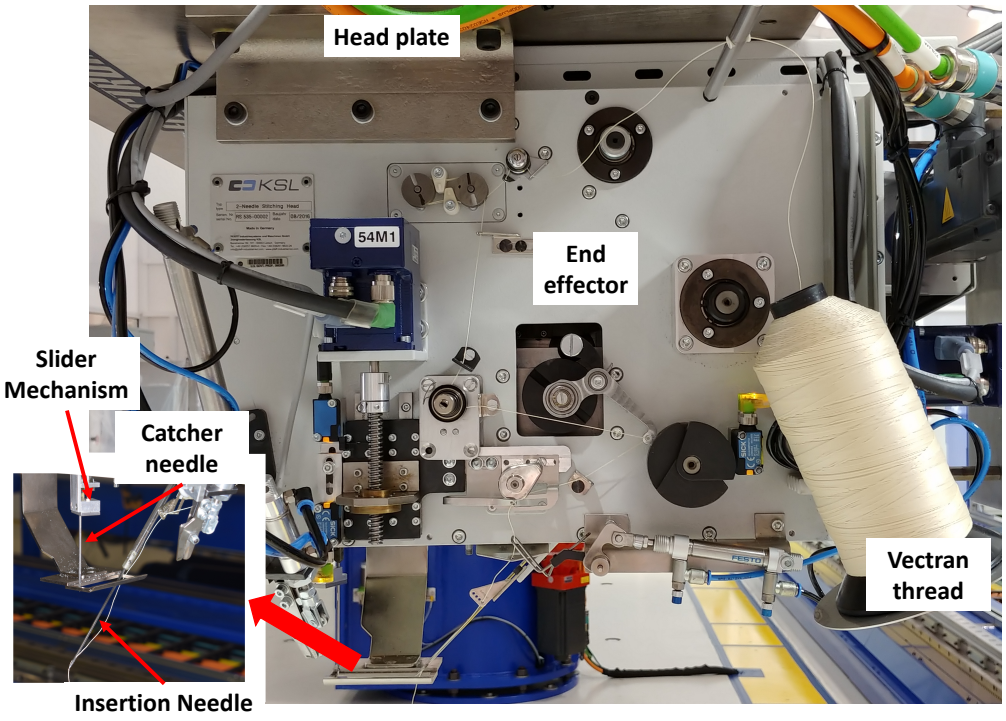


Figure 4. RS535 (single-sided) stitching head.

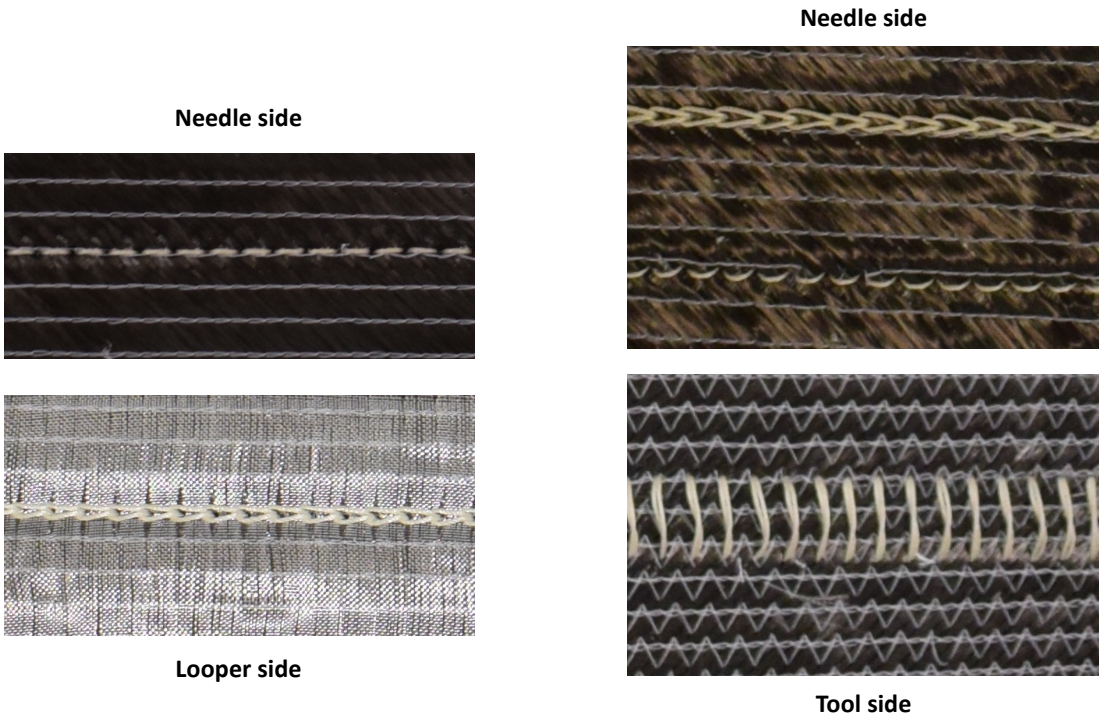


a) RS566 (double-sided) b) RS535 (single-sided)

Figure 5. Stitching patterns for the stitching heads.

# 3. STITCHING PATH DEVELOPMENT

When stitching operations are performed on ISAAC, a stitching head is placed on the robot, replacing the AFP head shown in Figure 2. Stitching is performed with the aid of a support structure for the fabric preform for double-sided stitching or a "stitch tool" for single-sided stitching. Either of these is typically attached to the coupon table. The robot is programmed to follow stitch paths that are consistent with support structure or grooves in the stitch tool that allow the needles to pass below the carbon fabric without touching the stitch tool itself. The geometry of the support structure or stitch tool is generally consistent with the desired shape of the final part. A further discussion of stitch tools is presented in Ref. 17.

As mentioned in the previous section, control for stitching paths during the manufacturing and installation process for the two stitching heads using ISAAC was limited to straight-line paths. This capability was consistent with the stitching that Boeing conducted during ERA, where paths consisted of a collection of short, straight-line stitching paths. Since future stitching activities are expected to require longer, 3D curved stitching paths in space, further stitching path development has been conducted to develop these 3D curved stitching paths. This section describes the stitching path development that has been accomplished. First, the description of the initial stitching path definition is presented to provide a baseline for stitching path definitions and programming. Next, the development and definition of the complex 3D stitching path in space, which is the primary focus of this paper, is presented. Lastly, some examples of 3D stitching paths requiring the new path definition are presented.

## 3.1 Initial Stitching Path Definition

The control for the stitching heads on the ISAAC system had to be developed from scratch since the LaRC stitching heads are placed on a different base robot compared to the robots that Boeing used in the ERA project, and they use different controllers and software. Development of the stitching control laws required definition of the "tool point" that is defined as the point associated with a head that controls the motion of the head.

The tool point is shown in Figures 6 and 7 for the double-sided and single-sided stitching heads, respectively. The control programming provides the ISAAC robotic system the information about the tool point and the required motion that guides the stitching head while traversing the stitching path. The tool point for the double-sided RS566 stitching head has been defined as the point where the needle pierces the top surface of the end effector table as shown in Figure 6. The preform is placed between the presser foot and the end effector table.

The tool point for the single-sided RS535 stitching head has been defined as the point on stitching tool surface where the catcher needle penetrates tool surface, as shown in Figure 7. The preform is placed between the stitching tool surface and the presser foot surface. During the stitching process, the end effector table supports the preform for double-sided stitching, while the stitching tool supports the preform for single-sided stitching. Note that the needle side shown in Figure 5b is the presser foot surface identified in Figure 7 and shown in Figure 8. Preforms with straight stitching paths have successfully been stitched using the ISAAC system with both the RS566 and RS535 heads.

A sketch of the presser foot surface stitch pattern for the RS535 head is shown in Figure 8, where the circles on the stitch pattern indicate the needle penetration points. In the figure the green lines represent thread placed by the insertion needed and the red lines represent thread placed by the catcher needle. The programmed stitch path is shown by the black line. As indicated in the figure, the lengths of the stitch patterns produced by the catcher and insertion needles are equal to the defined stitch length. Straight stitching paths have been used on curved preforms, but their use constrains the design space due to potential stitching problems.

An example of where the straight-line stitching path was successfully used for a curved preform is presented next. A close-up of a stringer/frame bay end on a cylindrical curved panel fabricated by Boeing (Ref. 10) using single-sided stitching is shown in Figure 9. The inner mold line (IML) or tool side is shown. The bay was bounded by the stringers on two sides parallel to the cylinder axis and the frames on the other two sides that were in the circumferential direction. Therefore, the frame webs were curved within their planes, and the flanges of the frames matched the curvature of the skin. The panel had an outer mold line (OML) radius of 90 inches with a stringer spacing of 7.8 inches and frame spacing of 24 inches. The stitch lines connected stringer and frame flanges to the skin within the bay end. Because the stich line on the frame flange does not extend to the stringer centerlines, the approximate length of the frame flange stitch line was about 5.4 inches. The frame flange path was stitched as a straight line in space. The straight line path led to the IML stitch width, the distance of the length of the stitching where the needles penetrated the IML, to be longer at the center of the path (indicated by orange line in Figure 9) than at the end of the path (indicated by red line in Figure 9). Despite this very small chord length, the difference in stitch width at the center and end of the stitch path was about 6%, and is noticeable in the figure where the orange and red stitch width lines are brought close together for comparison, with the blow up inset emphasizing that length difference. As the radius of a preform reduces or the arc length of the stitching path increases, this discrepancy in stitch path width increases and leads to difficulties with stitch formation. Therefore, stitching preforms along a small radius of curvature along a circumferential cylindrical path requires that the stitch path be defined as a 3D curve in space to enable proper stitch formation. The same difficulties arise for any curved stitching path in a plane in which the catcher needle lies throughout the entire stitching path, which is equivalent of the stitching head rotating about the x-axis of a coordinate system affixed to the stitching head at the tool point as shown in Figure 7. Therefore, a stitching path that contains rotation of the head about the x-axis of the local tool point coordinate system (shown in Figure 7) can create a stitch with an insufficient loop for the catcher needle to hook. The severity of the mal-formation is increased as the length of the stitching path increases and as the radius of the stitching path decreases. Additional, and more severe, stitching difficulties arise when the stitching path includes rotations of the stitching head about the local tool point coordinate system z-axis (see Figure 7). Therefore, improvement of the stitching path development and definition are required for generally curved stitching paths, which is presented in the next section.

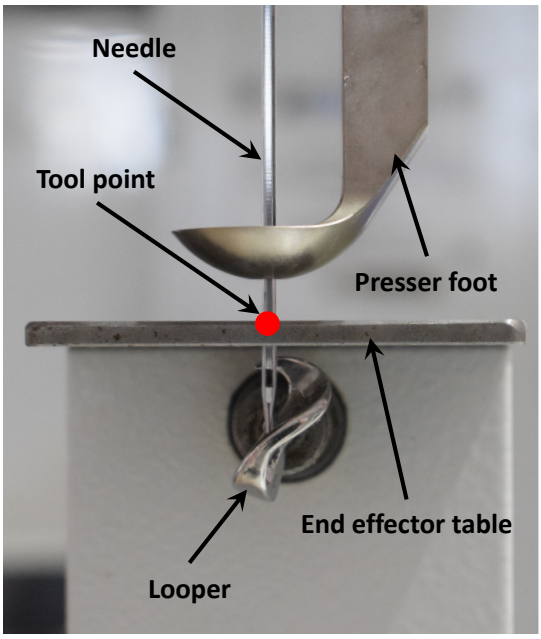


Figure 6. Tool point for the RS566 stitching head.

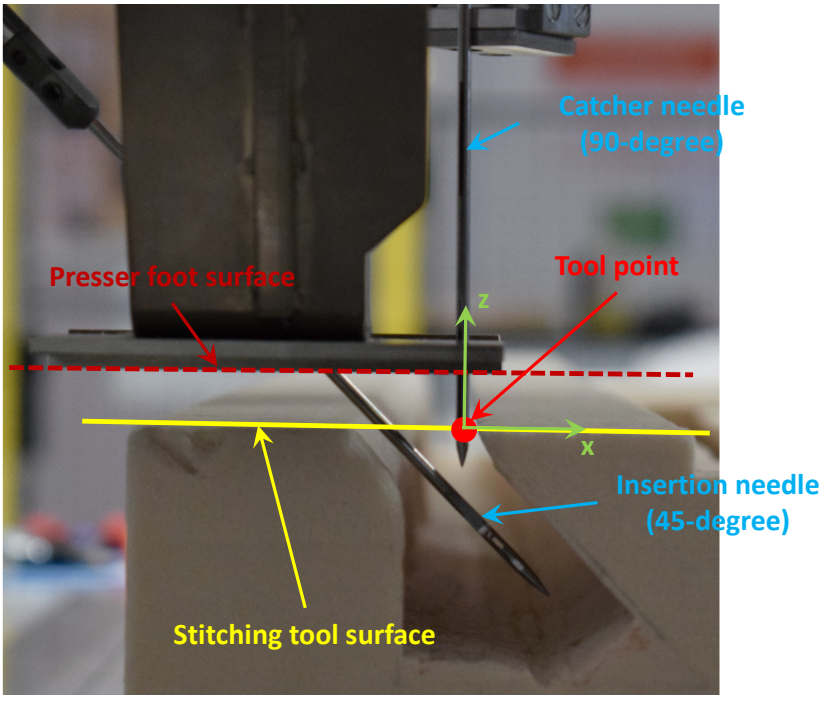


Figure 7. Tool point for the RS535 stitching head.

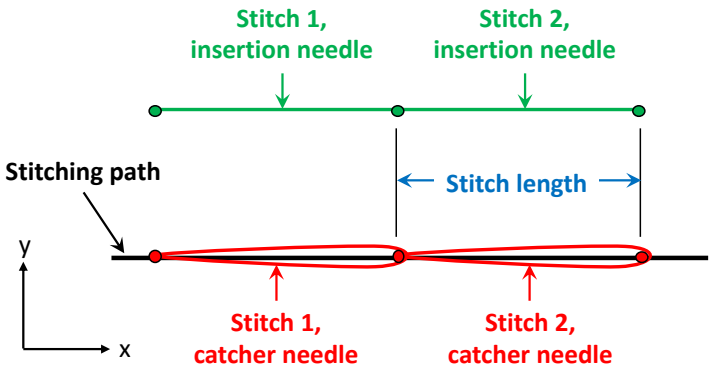


Figure 8. RS535 stitch pattern on the presser foot surface of the preform.

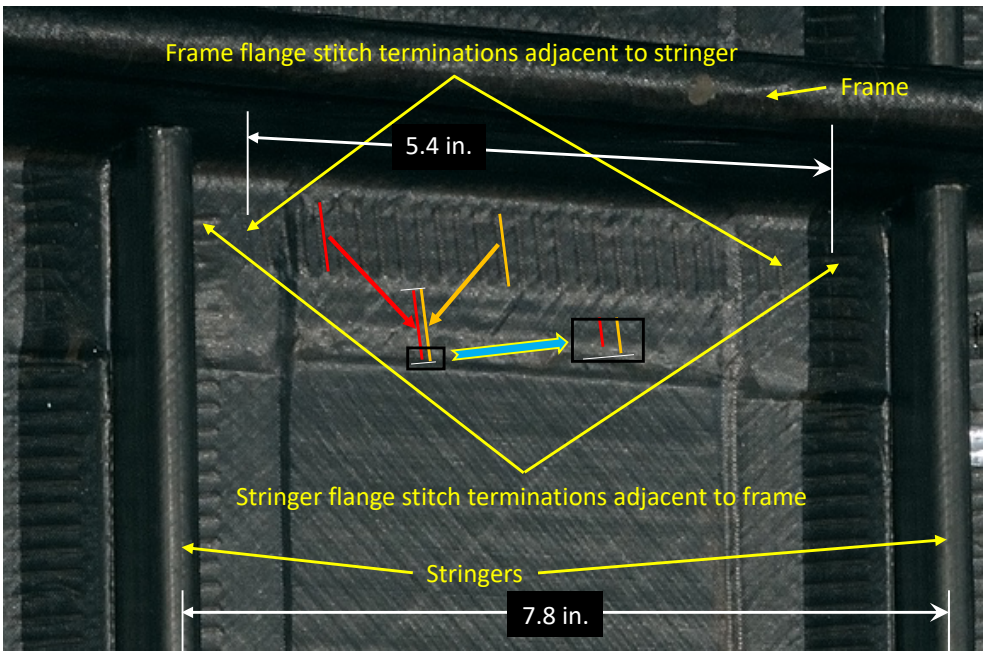


Figure 9. Stitch path terminations for frames and stringers in curved panel test article.

### 3.2 Path Definition Process

Developing 3D stitching paths consists of two basic steps, namely, 1) developing the stitching control logic, and 2) producing the required control programming. These two items are intimately related to each other, but the development of the paths is presented herein by first describing the logic by which the stitching is controlled, followed by the description of how that logic informs and dictates the control programming. Additionally, because the double-sided RS566 stitching head has only a single needle, it is less affected by the path curvature, and can be considered to be a subset of the single-sided RS535 stitching head as it applies to developing and defining the stitching path. Therefore, the remainder of this section focusses mainly on the RS535 stitching head, and where appropriate, how the RS566 relates to the RS535.

### *3.2.1 Effects of including path curvature (head rotations)*

An important consideration in understanding why the stitching path control is greatly affected by the curvature of the stitching path is to first understand the way that the stitching head works. Specifically, the motion of the needles during the stitching process are the key factor. As originally programmed, the stitching head traverses the stitching path continuously during the stitching process. However, the needles penetrate the material during the stitching process, and to avoid side forces on the needles, a needle walk mechanism moves the needles within the presser foot during the stitching process as shown in Figure 10. In the figure, the yellow line indicates the position of the two needles that can be seen to move within the presser foot, as indicated by the green arrows, in the opposite direction of the presser foot/head motion indicated by the red arrows. The amount of walk required depends on the length of the stitch, and for a typical 5-mm stitch length the needle walk is between 3.5 mm and 4.0 mm. For straight stitching paths, the walk ensures that the needles are not subjected to side forces during the stitching process. However, for a curved stitching path in space, side forces develop on the needles that increase with increasing rotations.

While following a curved stitching path, the stitching head rotates about the tool point around the three axes of the local tool point coordinate system shown in Figure 7. First, consider a stitching path where the only curvature is in the yz-plane, that is, a rotation about the x-axis. A rotation about the local tool point coordinate system x-axis has been discussed previously regarding a cylindrical panel. During this rotation, the catcher and insertion needles have the same translation and rotation throughout the stitching cycle. Therefore, the stitching pattern is the same as a straight seam shown in Figure 8 where both needles create a stitch pattern equal to the stitch length. Very little side force is exerted on the needles during this motion. However, stitch formation is affected because the distance between the catcher and insertion needles shortens on the stitching surface at the ends of the stitching path for a convex surface, and lengthens at the ends of the stitch path for a concave surface when a straight path is used. By introducing curvature to the stitching path by including x-axis rotation, the stitch formation problem exhibited by a straight path on the curved surface is eliminated regardless of the stitch path length or radius of curvature because the distance between the needle penetration points on the stitching surface remains the same.

Second, consider a stitching path that only rotates the stitching head about the local tool point coordinate system y-axis. Rotation about the y-axis tries to rotate the needles within the preform, but introduces small side loads on the needles. However, without including the rotation about the y-axis where the surface normal of the stitching surface does rotate, problems with stitch formation can occur. Stitch formation problems occur because the distance between the needle penetration points on the stitching surface can change dramatically for large rotations as shown in Figure 11. In the case where a rotation about the y-axis is not included in a stitch path, the stitch formation can have problems due to the thread loop being too small for the case shown in part b) of the figure, or too large if the rotation is in the opposite direction.

Third, consider a rotation about the local tool point coordinate system z-axis that creates a curved path in the xy-plane. For the RS535 stitching head we define a convex path as having the insertion needle on the convex side of the curve as shown in Figure 12a, and a concave path as having the insertion needle on the concave side of the curve as shown in Figure 12b. This stitching path motion results in a stitch pattern for the insertion needle that is much longer or much shorter than that of the catcher needle for convex and concave paths, respectively.

A difference in length is shown in Figure 13 for the two cases. The difference in stitch pattern length for the two needles results in a significant side force on the insertion needle during the stitching process. As previously noted, the needles are in the preform for a significant portion of the stitch formation process. The walk mechanism of the stitching head moves both needles the same translational distance, and therefore cannot alleviate the side force on the insertion needle for this curved path. This inability is because the tool point is on the catcher needle, so the walk mechanism controls the translation of the catcher needle the proper distance for the stitch length and keeps side forces off the catcher needle.

The rotation of the stitching head about the local tool point coordinate system z-axis imposes the most severe problems on the stitching process for the RS535 head. A means of controlling the stitching path, given the restrictions of the stitching head mechanisms, is necessary to alleviate the side forces on the insertion needle for a path containing rotation of the head about the local tool point coordinate system z-axis. Contrary to this, for the double-sided RS566 stitching head, a rotation about the local tool point coordinate system z-axis has no significant effect because such a motion simply results in a drilling motion of the needle and introduces no side forces or formation problems.

In summary, rotations about the local tool point coordinate system axes affect the two stitching heads if a path is curved in 3D space. A rotation about the local tool point coordinate system x-axis or y-axis imparts similar forces on the RS566 needle and the RS535 catcher needle, and the RS535 insertion needle also is subjected to side forces. In addition, the stitch formation for the RS535 can be affected if a straight path without rotation included is used on a curved surface. If these rotation-induced shortening or lengthening of the distance between the catcher and insertion needle penetration points on the stitching surface leads to improper loop formation for the catcher needle to hook the thread.

A rotation about the local tool point coordinate system z-axis does not impart a force on the RS566 needle and the RS535 catcher needle, however, the RS535 insertion needle can be subjected to significant side forces due to the increased or decreased translation resulting from the rotation. Stitching a series of straight segments for a curved path within the tool point coordinate system xy-plane is not practical, since this series of straight segments would not be a smooth stitched path. Special programming is necessary to stitch a curved path with rotation about the z-axis and for general paths that require rotations about all three tool point coordinate system axes. The method for developing the curved stitch paths in space is presented next.

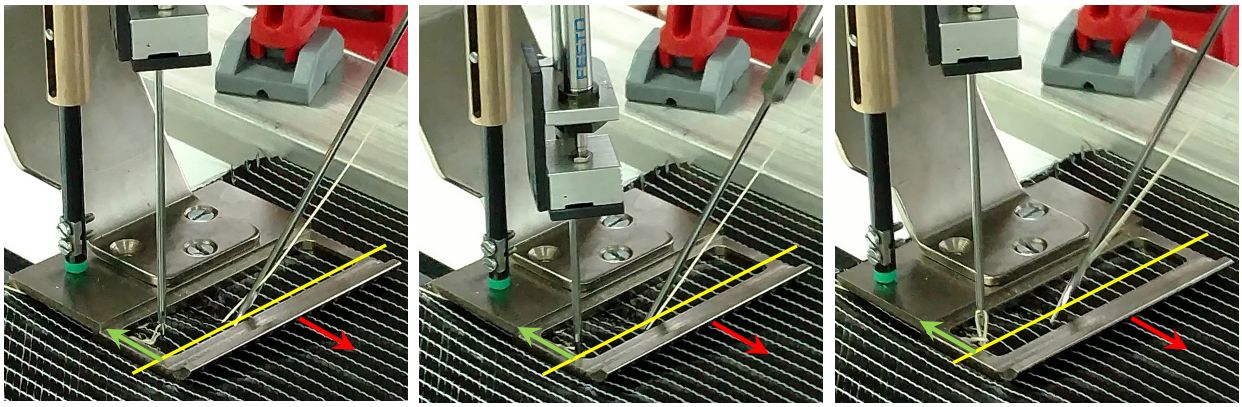

a) At needle insertion b) During stitch c) At needle retraction

Figure 10. Needle walk evidenced by yellow line between needles traversing within presser foot (green arrow) as head moves along material (red arrow).

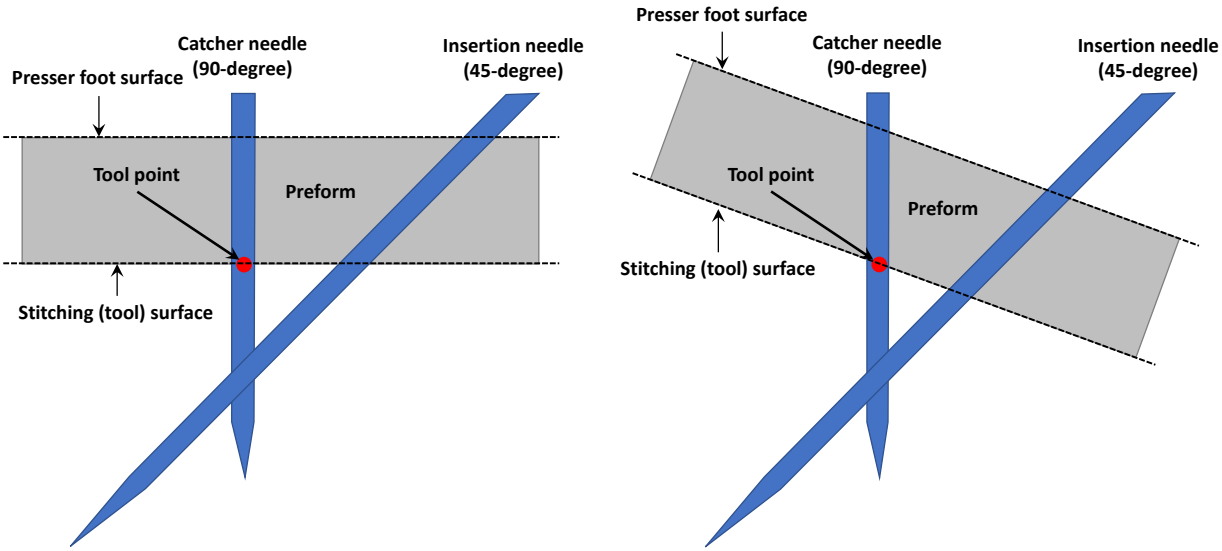


a) Starting orientation of path b) Without head rotation along path

Figure 11. Effect of not including a rotation about the tool point coordinate system y-axis.

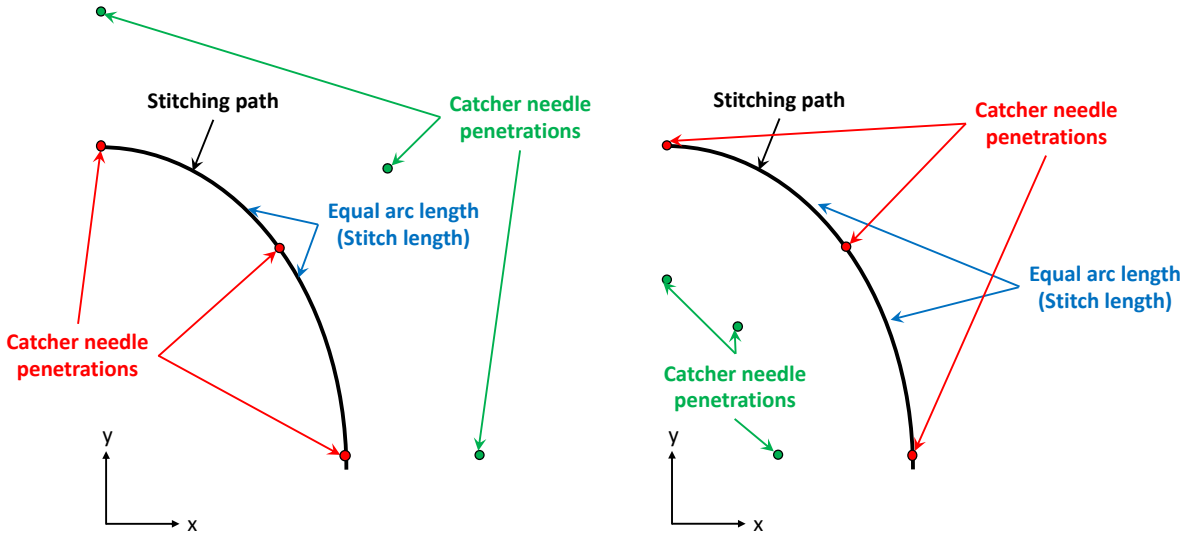


a) Convex path b) Concave path

Figure 12. Definition of convex and concave stitching paths for RS535 stitching head with head rotation about tool point coordinate system z-axis.

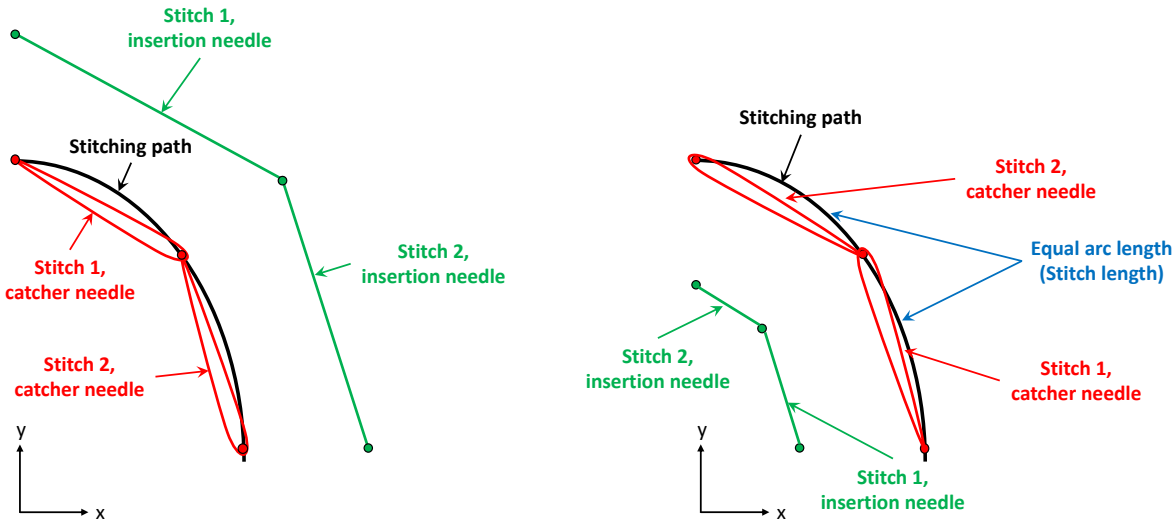


a) Convex path b) Concave path

Figure 13. Stitch patterns for RS535 stitching head with head rotation about tool point coordinate system z-axis.

### *3.2.2 Curved stitching path programming*

The control programming, or G-code, provides information by which the robotic system carries out the stitching process. In general, the preprocessor provides location information along a curve

for the tool point to follow and the points output by the preprocessor are more than sufficient to determine a unique path for the tool point to follow. The total distance travelled along the stitching path and a parameter that is tied to the rotation of the drive motor for the stitching head are included with the position points. The drive motor operates cams that complete the stitching process such as needle movement, needle walk, thread tension, and numerous other operations during a full revolution. The drive motor is synchronized with the path motion such that the drive motor completes a single rotation for each stitch length portion of the stitching path traversed by the tool point. As programmed for straight stitching paths, the number and spacing of points to define the curve is not important, and the control system matches the distance along the stitching path with the positions along the path at which the drive motor is to complete revolutions. While this system works for the straight stitching paths, this system does not work for curved stitching paths in 3D space.

In addition to point locations, path length and stitching drive motor information, head rotations in the global coordinate system are specified for curved paths in space. For non-stitching heads, such as the AFP and ultrasonic cutting knife, the preprocessor output controls the head motion satisfactorily because they are only dependent on putting the tool point at a certain location. To control the total motion of the ISAAC heads, the control system interpolates between the programmed points, with the head controlling the tool point to traverse the specified path while rotating the head at the same time. The output currently provided by the preprocessor does not work for stitching curved paths because of the problems associated with rotating the stitching head while the needles are in the preform. Therefore, a method to prevent the problems associated with stitching while applying continuous translations and rotations simultaneously along the stitching path was developed.

Two main considerations informed the choice of how to produce a stitching path definition that permits the proper stitching process along the path. First, the stitch path is not dependent upon the complete path curve, but rather only upon the starting and ending points of each stitch, that is, the locations where the needles penetrate the preform. This requirement is contrary to other heads like the AFP head and ultrasonic knife that must traverse the entire path while being in contact with the part. Second, since the needles cannot be in the preform while the head is rotating, rotations must occur in the parts of the stitching process when the needles are not in the preform. To accomplish this feat, the translation and rotation for each stitch were decoupled. In terms of programming, this decoupling resulted in only the end points of each stitch being defined, and the rotations being applied at the end of each stitch after the translation has been completed. The process for determining the points and rotations is provided next.

The process for developing the stitching path definition and G-code development is depicted in Figure 14. The process begins with input of the stitching surface, stitching path curve (curve the tool point will follow) and the nominal stitch length ($l_{s,n}$). It is desirable for a stitching path to have an integer number of stitches, so a stitch length for the path is calculated for the integer number of stitches that provides a stitch length closest to the nominal stitch length ($l_s$). As the length of the stitching path increases, the difference between the path-calculated stitch length and the nominal stitch length decreases, and in general the difference between nominal and calculated stitch lengths is negligible. Points along the stitching path are extracted that are separated by equal arc lengths that are defined to be equal to $l_s$. This definition guarantees that each stitch has the same length along the path, but results in the loop produced by the catcher needle to be equal to (for straight

segment) or shorter than (curved segment) the stitch length since the catcher needle is coincident with the tool point and the end points represent a chord of the curved path. The length of the insertion needle stitch pattern depends on whether the curve is convex or concave as discussed previously.

Each stitch progresses from its starting point to the ending point, which is the starting point for the next stitch (with the exception of the last stitch that ends at the stitching path end point). Using the set of calculated stitch points, a direction vector ($\boldsymbol{V}_i$) for each stitch is calculated. This direction vector is coincident with the local tool point coordinate system y-axis and represents the direction that the stitching head will traverse during the stitch cycle for each stitch. In addition to the orientation vector for each stitch, the tool point coordinate system z-axis and x-axis orientations are calculated for each stitch at the stitch starting point, with the z-axis being coincident with the surface normal at the stitch starting point. The local tool point coordinate system axis vectors are defined in the global coordinate system used by the control system to control the head motion during the stitching process. Given the stitching path starting point and the local tool point coordinate system for the first stitch, the translational and rotational positions for the head at the start of the stitching process for the stitch path are calculated.

Programming begins by writing out the code for the stitching path starting point calculated translational and rotational positions. Also, written out on each line of code are the cumulative path length and the drive axis distance that are both set to zero for the starting point. The drive axis distance is defined as a distance that identifies when full rotations of the drive motor occur, when provided a stitch length. That is, the drive motor to completes a full rotation, and therefore operates the stitching mechanism through an entire stitch formation process, when the drive axis distance increments by the stitch length. Programming continues for each stitch by defining the code for the end point of the stitch (path ending point for the last stitch) and consists of two lines of code for each stitch. Prior to writing out the two lines of code for a stitch, the Euler angles required for rotating the local tool point coordinate system at the starting point of the current stitch to be coincident with the local tool point coordinate system at the starting point of the next stitch are calculated. These Euler angles represent the total rotation of the head that occurs from the start of the stitch to the end of the stitch. Next, the first line of code for a stitch consists of the global translational position of the stitch end point replacing the values in the previous line of code. The rotational position values on the first line of stitch code are identical to the previous line of code, indicating that only translation of the head occurs with no rotation. The drive axis and the stitching path distances on the first line of stitch code are incremented by the stitch length, so that for the $n^{th}$ stitch, the drive axis and stitching path cumulative distances are defined as $n \times l_s$. The second line of code is written out with the translational position values, the drive axis distance and the stitching path distance equal to those on the first line of stitch code. The rotational positions of the second line of stitch code are calculated by adjusting the rotational values on the first line by the calculated Euler angles for the stitch. The second line of code is purely a rotation of the head after the stitch translation occurs in order to line up the head for stitching of the next stitch. Therefore, the two lines of code represent the uncoupling of the stitch translation that occurs in the first line of stitch code and the total rotation of the stitch that occurs in the second line of stitch code. Generation of these two lines of code for each stitch progresses until the final stitch lines of code are generated.

The process described provides the coding necessary to decouple the translation and rotation for each stitch to ensure that the problems associated with rotations of the head while the stitching needles are in the preform do not occur. During the course of stitching trials, it has been seen that if the curvature is shallow (large radius), the problems do not manifest to a degree to raise concern. Thus, these shallow curved stitching paths can be stitched without difficulty using the control programming produced by the existing preprocessor, and decoupling of translations and rotations for each stitch are not required. Avoiding decoupling the translations and rotations is advantageous because executing the single line of code versus the two lines of code is faster. However, the described process enables the stitching when the curvature does require decoupling of the translation and rotation. Determining when to use the decoupled approach is part of ongoing stitching trials and is highly dependent on the rotation about the local tool point coordinate system z-axis for the stitch.

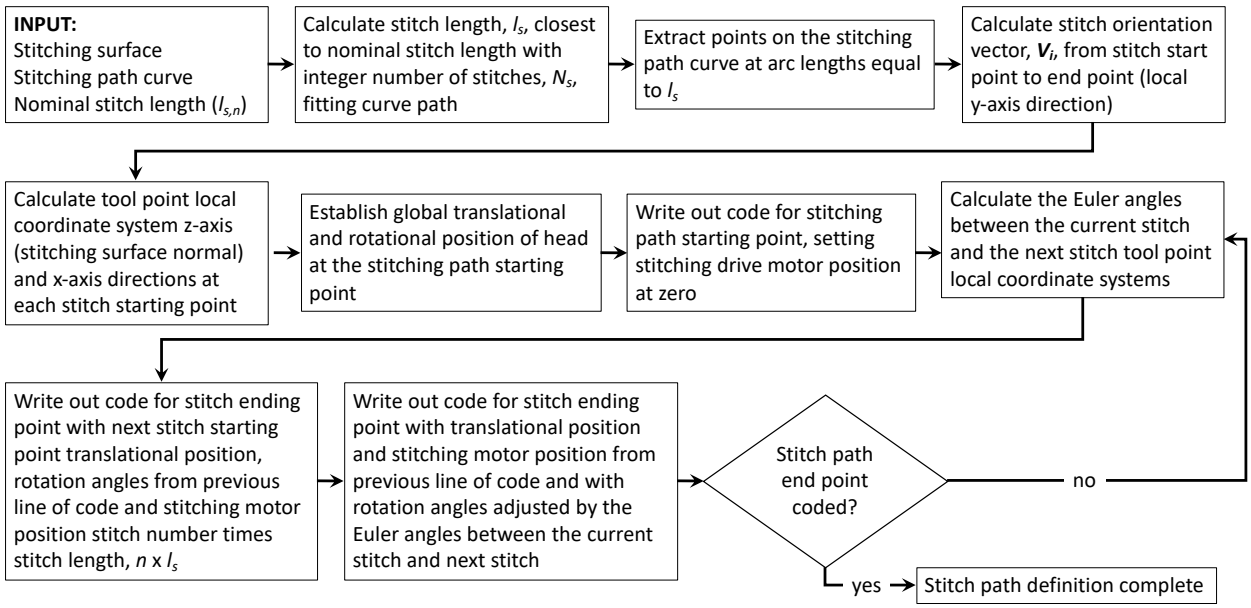


Figure 14. Stitching path development process flow chart.

### 3.3 Example Stitched Paths

Several stitching paths are presented to demonstrate when decoupling of the translation and rotation are necessary to produce 3D stitched paths. a closed planar circular path with an 8-inch radius is shown in Figure 15. To stitch this path, it was necessary to use the presented decoupling method, and preliminary information indicates that using the decoupled approach is preferable when the radius of curvature is less than 24 inches. A closed path is shown in Figure 16 that consists of straight edges that are connected using elliptical arcs with 1-inch radii where the ellipse segments meet the short ends of the shape. This type of path is representative of an access cutout in a wing lower skin. The stitching can be used to attach reinforcement to the cutout and to provide damage tolerance around the cutout. To stitch this path, the straight segments were not decoupled, but the elliptical segments were decoupled using the presented method. Lastly, a curve on a preform representative of the shape of the NTF wind tunnel blade is shown in Figure 17. For this

demonstrator, the two main path segments did not require decoupling of the translation and rotation, but the rotation that occurred between the two main segments was decoupled from the two paths. Other, more severe paths on the same demonstrator article do require decoupling of the stitch translations and rotations.

Figure 15. Closed, planar, circular path.

Figure 16. Closed path with straight and elliptical segments.

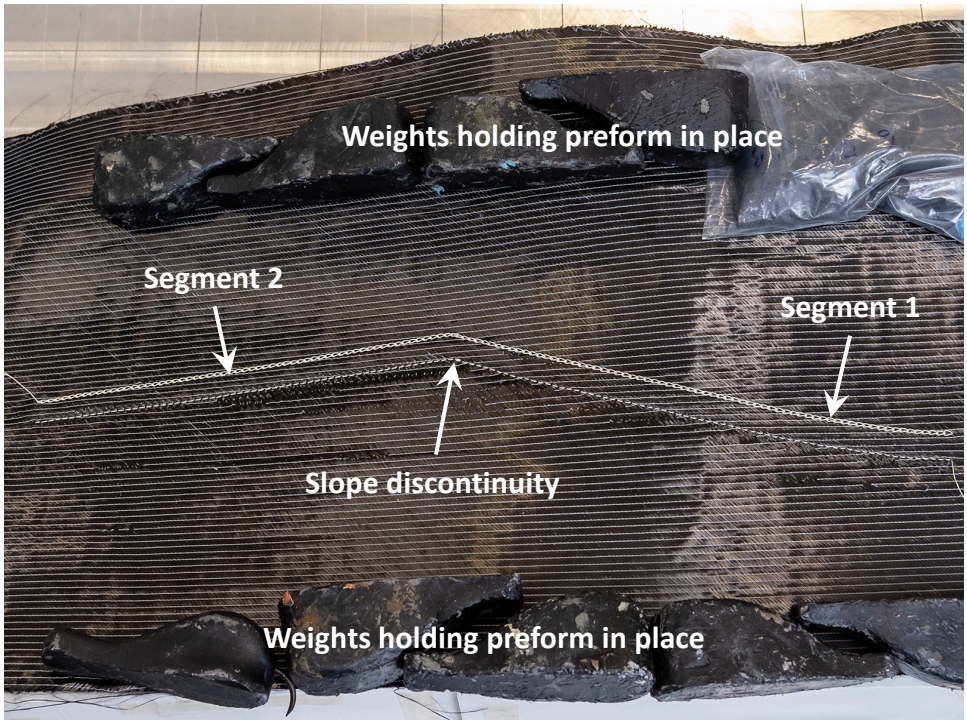


Figure 17. Two views of doubly-curved path demonstrator article representative of the NTF wind tunnel blade.

## 4. CONCLUSIONS

Stitching capabilities have been incorporated into the ISAAC system at NASA LaRC through the introduction double-sided and a single-sided stitching heads. Initial stitching path control was implemented as straight lines in space as was done for previous stitching development. However, more complex stitched structures such as a wind tunnel blade or cutouts within a fuselage or wing skin require that the stitching paths be implemented as 3D stitching paths in space. Unfortunately,

current control programming output by a preprocessor where translations and rotations are applied to the head motion simultaneously cannot stitch these curved paths due to problems that arise in stitch formation and the introduction of side forces on the needles. This inability to stitch is most pronounced for the single-sided stitching head, where two needles are in the preform at the same time for the majority of the stitching process. A means to program 3D stitching paths in space was developed whereby the translation and rotation of each stitch were decoupled, thereby eliminating the problems associated with current control programming approaches. Using this newly developed stitching path definition and control programming, complex stitching paths have successfully been stitched at the ISAAC facility. In order to mitigate the time penalty that is associated with decoupling the stitching path motion, research is ongoing to develop rules to determine when this translation and rotation decoupling method should be applied.

## 5. ACKNOWLEDGEMENTS

The authors wish to thank Mr. Patrick J. Thrash of The Boeing Company for his valuable contributions to the development of the stitching heads and their installation at the LaRC ISAAC facility.

## 6. REFERENCES

1. A. P. Mouritz, “Tensile Fatigue Properties of 3D Composites with Through-Thickness Reinforcement,” Composites Science and Technology, Vol. 68, 2008, pp. 2503-2510.
2. M. B. Dow and H. B. Dexter, “Development of Stitched, Braided and Woven Composite Structures in the ACT Program and at Langley Research Center (1985 to 1997),” NASA TP-97-206234.
3. D. C. Jegley, H. G. Bush, and A. E. Lovejoy, “Structural Response and Failure of a Full-Scale Stitched Graphite–Epoxy Wing,” Journal of Aircraft, Vol. 40, No. 6, November–December 2003, pp. 1192-1199.
4. M. Rouse, D. C. Jegley, D. M. McGowan, H. G. Bush, and W. A. Waters, “Utilization of the Building-Block-Approach in Structural Mechanics Research,” 46th AIAA/ASME/ASCE/AHS/ASC Structures, Structural Dynamics & Materials Conference, 18 - 21 April 2005, Austin, Texas. (Available as AIAA Paper 2005-1874.)
5. M. Karal, “AST Composite Wing Program – Executive Summary,” NASA CR-2001-210650.
6. K. Gould, A. E. Lovejoy, D. C. Jegley, A. L. Neal, K. A. Linton, A. C. Bergan, and J. G. Bakuckas, Jr., "Nonlinear Analysis and Experimental Behavior of a Curved Unitized Stitched Panel" Journal of Aircraft, Vol. 52, No. 2, March–April 2015, pp. 628-637.
7. D. C. Jegley, “Structural Efficiency and Behavior of Pristine and Notched Stitched Structure,” presented at the annual SAMPE meeting October 17-20, 2011.
8. N. Yovanof and D. C. Jegley, “Compressive Behavior of Frame-Stiffened Composite Panels,” presented at the 52nd AIAA Structures Dynamics and Materials Conference, April, 2011.
9. D. C. Jegley, “Behavior of Frame-Stiffened Composite Panels with Damage,” presented at the 54th AIAA Structures, Structural Dynamics, and Materials Conference, April, 2013.

10. A. Allen and A. Przekop. 2012. “Vibroacoustic Characterization of a New Hybrid Wing-Body Fuselage Concept,” presented at the INTER-NOISE 2012 Conference, August, 2012.
11. A. E. Lovejoy, M. Rouse, K. Linton, and V. Li, “Pressure Testing of a Minimum Gauge PRSEUS Panel,” presented at the 52nd AIAA Structures Dynamics and Materials Conference, April, 2011.
12. N. Yovanof, A. E. Lovejoy, J. Baraja, and K. Gould, “Design Analysis and Testing of a PRSEUS Pressure Cube to Investigate Assembly Joints,” Aircraft Airworthiness and Sustainment Conference, April, 2012.
13. A. Przekop, “Repair Concepts as Design Constraints of a Stiffened Composite PRSEUS Panel,” presented at the 53rd AIAA/ASME/ASCE/AHS/ASC Structures, Structural Dynamics and Materials Conference, May, 2012.
14. A. Przekop, D. C. Jegley, M. Rouse, and A. E. Lovejoy, “Analysis and Testing of a Metallic Repair Applicable to Pressurized Composite Aircraft Structure,” Presented at the Society for the Advancement of Material and Process Engineering (SAMPE)Technical Conference, June, 2014.
15. D. C. Jegley, “Experimental Behavior of Fatigued Single Stiffener PRSEUS Specimens,” NASA-TM-2009-215955.
16. P. J. Thrash, “Manufacturing of a Stitched Resin Infused Fuselage Test Article,” Presented at the Society for the Advancement of Material and Process Engineering (SAMPE) Fall Technical Conference, Orlando FL, October, 2014.
17. R. A. Wahls, “The National Transonic Facility: A Research Retrospective,” AIAA Paper 2001-0754, 39th AIAA Aerospace Sciences Meeting and Exhibit,” January 8-11, 2001, Reno, Nevada.
18. R. M. Grenoble, R. Harik, D. M. Munden, J. Halbritter, D. C. Jegley, and B. H. Mason, “Assessment of Automated Fiber Placement for the Fabrication of Composite Wind Tunnel Blades,” Proceedings of Society for the Advancement of Material and Process Engineering (SAMPE) 2019 Conference and Exhibition, Charlotte, North Carolina, May 20-23, 2019.
19. R. Harik, J. Halbritter, D. C. Jegley, R. W. Grenoble, and B. H. Mason, “Automated Fiber Placement of Composite Wind Tunnel Blades: Process Planning and Manufacturing,” Proceedings of Society for the Advancement of Material and Process Engineering (SAMPE) 2019 Conference and Exhibition, Charlotte, North Carolina, May 20-23, 2019.
20. B. H. Mason, D. M. Munden, D. C. Jegley, R. W. Grenoble, and R. Harik, “Design and Analysis of a Tool for Automated Fiber Placement of Composite Wind Tunnel Blades,” American Society of Composites (ASC) 34th Technical Conference, Atlanta, GA, September 23-25, 2019.
21. NASA ISAAC Fact Sheet, FS-2016-12-273-LaRC, 2016.
22. https://www.cgtech.com/ Accessed 12/17/2018.